

Effects of Oscillating Plates on the Plane Mixing Layer, Its Developing Region and Jet

M. Ichimiya

Department of Mechanical Engineering
University of Tokushima, 2-1 Minami-Josanjima, Tokushima 770-8506, JAPAN

Abstract

Effects of oscillating plates on the plane mixing layer, its developing region and jet were experimentally investigated. The flow was formed by the jet issued from the two-dimensional nozzle and surrounding quiescent air. Two plates oscillate perpendicularly in relation to the main flow. Mean and fluctuating velocity components and Reynolds shear stress component were measured by hot-wire anemometers. With the disturbance of the plate, self-preservation was promoted and the width of the layer was enhanced. The transition process with the disturbance was enhanced by an interaction of the inherent periodic variation and the disturbance induced by the plate.

Introduction

A jet is a fundamental flow that occurs widely in the natural world and industrial machinery. It is important to understand its characteristics and properties. Many studies have been reported on it for a long time. Among others, there are many studies which introduced various kinds of disturbance in laminar jet and sought to cause the transition to turbulence.

In free shear flows such as a jet, in the transition process a periodic disturbance appears at first, then the harmonics and subharmonics appear, and finally an irregular disturbance dominates. In power spectrum distribution, a large peak appears, then many maximum values gradually appear, and finally maximum values disappear. The development process of this disturbance is divided into the linear region when disturbance amplifies exponentially, the nonlinear region where harmonics and subharmonics of the fundamental wave appear and an irregular region where irregular fluctuation dominates. Exponentially increasing velocity fluctuation in space [8] and time [9] was analyzed by Michalke. Freymuth confirmed the analysis by his experiment [2]. Due to the sensitivity of spatially-developing shear flow to the outer disturbance, outer forced disturbance was added to jets or mixing layers, and then many studies in which the disturbance to increase instability or promote transition were carried out.

In the study of forced transition, experiments have been performed to introduce a periodic disturbance with a frequency approximately equal to the fundamental frequency occurring in the natural transition process. An additional style of the disturbance is roughly classified into the one in which a speaker produces a sound wave disturbance [1,2,5,6,7,10,11,12] and another in which a flap or ribbon is oscillated [3]. A successful method was introduced by which a forced disturbance whose frequency was approximately the same as the fundamental frequency of the flow promoted a turbulent transition. But few experiments have been conducted in which the disturbance frequency was considerably different from the fundamental one. Therefore, in the present study, a disturbance of 5 Hz is introduced which is two orders of magnitude lower than the

fundamental frequency. To produce such a low-frequency disturbance, an oscillating device is more appropriate than a sound wave.

In the oscillation method, the disturbance position is controlled by the device, though in the sound method the disturbance is introduced to the whole flow field. The oscillation method is suitable to follow spatial development of the disturbance. In this method, rotary flat plates, vibrating ribbons, and oscillating flaps were used. The rotary flat plates and the vibrating ribbons change the attack angle, thereby changing lift and circulation, so that vortices are shed. In the method to push out a plate perpendicular to the flow, separated vortices from the plate are shed. Therefore, in this study, perpendicularly oscillating plates are installed at the exit of the two-dimensional jet. Then, laminar-turbulent transition of the mixing layer, which is formed between the jet and surrounding quiescent air, was examined. At first, this kind of disturbance will be specified, and the flow which occurs by periodic oscillation will be clarified. Then, how the self-preservation process is affected by the disturbance will be clarified.

Experimental Apparatus and Methods

A wind tunnel of blowing type was used in this study. Air is blown into the measurement section from a two-dimensional nozzle exit of aspect ratio 31 (310 mm in width and 10 mm in height). The flow at the exit has velocity gradient within 1 mm from upper and lower nozzle walls, respectively. While the velocity is kept constant in the middle region of the height, 8mm. Two side walls 310 mm apart from each other for a whole measurement section were installed to secure the two-dimensionality of the flow. Two oscillation plates 2 mm in thickness are then installed across the whole width to give a disturbance. The plates oscillate sinusoidally in relation to the flow at a frequency, f_d , of 5 Hz. This frequency is two orders of magnitude smaller than the fundamental frequency in the natural transition process, which is, approximately, 500 kHz. The flow field and coordinate system are shown in Figure 1. The lower

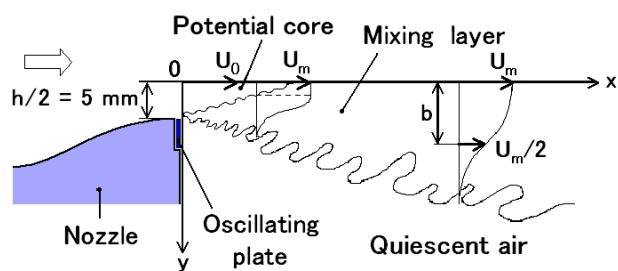


Figure 1. Schematic diagram of two-dimensional mixing layer and coordinate system

half of the flow field is shown in the figure. The top of the oscillating plate shown there becomes flush with the nozzle wall surface when it descends to its lowest point, and then rises by 0.25 mm from the surface at most. This value was chosen so that no disturbance from the separation of the flow occurred. The Strouhal number based on this value, plate oscillation frequency f_d and nozzle exit velocity U_0 , are about 1.7×10^{-4} . In addition, another oscillating plate is installed in the upper half of the flow field in symmetry with respect to the nozzle centerline, $y = 0$. The plate oscillates symmetrically with the former plate. In other words, the nozzle height 10 mm is decreased 0.5 mm at the moment when the two plates protrude maximally from the nozzle respective surfaces. The motor revolution is transmitted to two cams by belts, and then the revolution of each cam is transmitted to the protrusion of each oscillating plate. The noise of the motor and cams were checked and confirmed not to affect the flow transition. A photo sensor signal corresponding to the angle of rotation of this cam is the output, and the phase of the plate oscillation is detected. Two types of experiments were performed. In one, the plates remain stationary so that the oscillating plates do not narrow the nozzle exit section (without disturbance). In another, the plate oscillated at a frequency of 5 Hz (with disturbance). In any case, the Reynolds number based on the nozzle exit velocity, U_0 , and nozzle exit height, h , was 5000. Experiments were conducted at a spanwise position, $z = 20$ mm, where the velocity distribution becomes almost symmetric with respect to the centerline, $y = 0$.

X-shaped hot-wires with a diameter of 5 μm and 1 mm in length were used for the measurement, and the output voltage was sampled at a sampling frequency of 5 kHz for about 52 seconds. This interval is equivalent to about 260 periods of oscillation when the plates oscillate. The measurements were conducted in a range of $y \geq 0$.

Results and Discussion

Aspect of Disturbance Just After Nozzle Exit

At first, an aspect of the disturbance just after the nozzle exit will be described.

In Figure 2, the respective differences of the ensemble-averaged and time-averaged velocities of the streamwise and normal directions, $\langle u \rangle$ and $\langle v \rangle$, are shown at several normal positions.

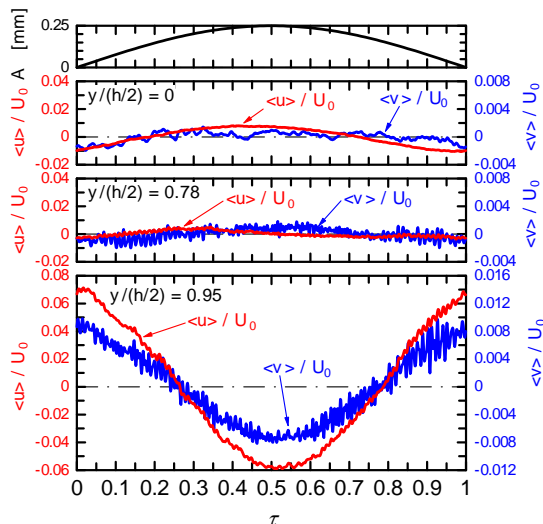


Figure 2. Ensemble-averaged velocity signals just downstream of nozzle, $x/h = 0.5$

The uppermost figure shows the displacement of the oscillating plates. The phase $\tau = 0$ and 1 correspond to the instant when the plate does not narrow the nozzle section at all. The phase $\tau = 0.5$ corresponds to the instant when each plate protrudes 0.25 mm and narrows the nozzle cross section 5% in total. There is a potential core region in the nozzle centerline neighborhood just after a nozzle exit, as will be mentioned later in figure 4. At this $x/h = 0.5$, the potential core reaches from $y/(h/2) = 0$ to approximately 0.8. At first, in $y/(h/2) = 0$ streamwise velocity, $\langle u \rangle$ changes by the same period as the oscillation. The negative absolute value becomes the maximum, i. e., the ensemble averaged value $U + \langle u \rangle$ becomes the smallest at $\tau = 0$, when the oscillating plates do not narrow the nozzle cross section at all. The value becomes a positive maximum, i. e., the ensemble averaged value becomes the largest in the vicinity of phase $\tau = 0.5$ so that the plate narrows the nozzle cross section most. In other words, the ensemble averaged velocity increases or decreases in correspondence with the decrease and increase of the nozzle cross section. A ratio of the minimum and the maximum values is about 0.98. This value is close to the ratio of the minimum and the maximum of the nozzle exit cross-sectional area, 0.95. The normal velocity, $\langle v \rangle$, also changes by the same period, although the change is smaller than $\langle u \rangle$. It is difficult for the normal velocity fluctuation to reach this position. In addition, fluctuations of small amplitude can be seen in both velocity components, because this position is in the potential core. At $y/(h/2) = 0.78$, a change of $\langle u \rangle$ with the phase becomes smaller. The maximum and minimum values reach $\tau \approx 0.3$ and 0.8, respectively. This position exists in the border between the potential core and the mixing layer. Closer to the nozzle edge, at $y/(h/2) = 0.95$, the aspect of the change of $\langle u \rangle$ with the phase reverses, i. e., the velocity becomes maximum when τ is approximately 0, and minimum when τ is approximately 0.5. At $\tau = 0$ the value of $\langle v \rangle$ at first becomes maximum, i. e., when the plates are farthest away from the centerline, the normal velocity component is largest when furthest away from the centerline. On the other hand, the reverse is true at $\tau = 0.5$. The influence of plate oscillation appears most remarkable in this position. The change of $\langle u \rangle$ with the plate is almost the same as $\langle v \rangle$, i. e., opposite to the change of $\langle u \rangle$ at $y/(h/2) = 0$. In this way, the phase change of $\langle u \rangle$ reverses between the nozzle center and edge. This phase reversal will make the flow rate constant regardless of the phase. To check the preservation of flow rate, the velocity is integrated over the whole nozzle area. The ratio of flow rate and time-averaged rate, $Q(\tau)/Q_0$ becomes 1.00 for both $\tau = 0$ and 0.5 within the accuracy of the present measurement. Thus, the flow rate is kept constant in all phases in this way.

As described above, the phase variation of 5 Hz changes with the normal position, y . The power spectrum density of fluctuating velocity in the streamwise direction at the frequency of 5 Hz is

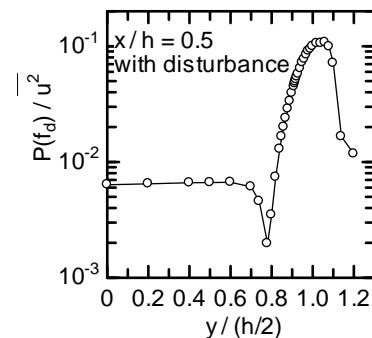


Figure 3. Power spectrum at plate oscillation frequency

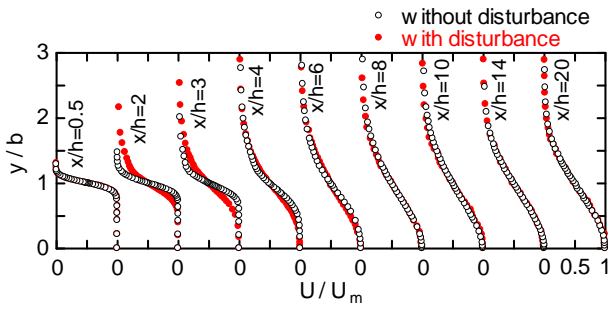


Figure 4. Mean velocity profiles

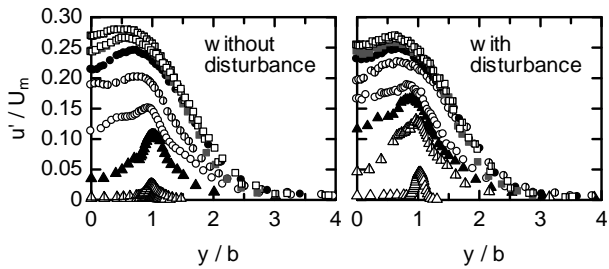


Figure 5. Distributions of streamwise fluctuating velocity: \triangle , $x/h = 0.5$; \triangleleft , $x/h = 2$; \blacktriangle , $x/h = 3$; \circ , $x/h = 4$; \odot , $x/h = 6$; \bullet , $x/h = 8$; \square , $x/h = 10$; \boxplus , $x/h = 14$; \blacksquare , $x/h = 20$

shown in Figure 3 against the normal position. The spectrum is constant until $y/(h/2) = 0.7$, then it decreases and reaches minimum at $y/(h/2) = 0.78$. This accords with the experimental result of Sato [12] in which the phase reverses in the position at which the power spectrum becomes minimum.

Completion of Similarity in Downstream Region

In this section, the developing process of self-similarity will be described.

The symmetry of the velocity distribution with respect to the jet centerline is an important problem. In this study, however, the region which is not affected by the other side is important, so the measurement was conducted only in a range of $y/b \geq 0$. Sato also indicated that the characteristics of one side of the plane jet have nothing to do with the other [12].

Figure 4 shows the streamwise mean velocity profiles. The normal position, y , is normalized by the half width, b , and the mean velocity, U , is normalized by the local centerline velocity, U_m . Profiles with and without disturbance coincide well at $x/h = 0.5$ just after the nozzle exit. Downstream, the potential core reduces and finally disappears at $x/h = 6$ and 3 without and with the disturbance, respectively. Further downstream, the mixing layer widens, in which the velocity gradient exists. The distribution becomes similar at $x/h = 10$ and 8 without and with the disturbance, respectively. In this way, the disturbance promotes the development of the jet. After the shape becomes similar, the shape is the same in both cases.

Figure 5 shows distributions of rms value of the fluctuating velocity in the streamwise component. Downstream, in both cases, the values generally increase, and the position y/b at which the value reaches maximum moves to the center, $y/b = 0$. This position of y/b almost coincides with the position where velocity gradient $\partial(U/U_m)/\partial(y/b)$ becomes maximum in the mean velocity

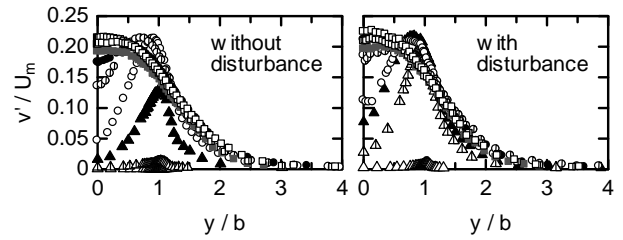


Figure 6. Distributions of normal fluctuating velocity: Symbols are same as Fig. 5.

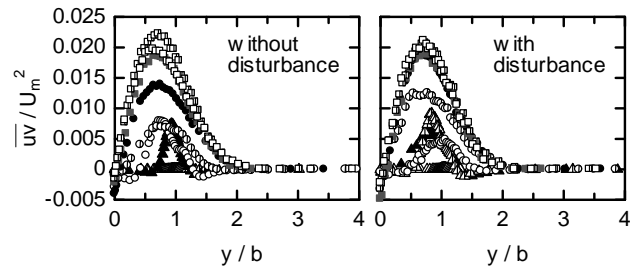


Figure 7. Distributions of Reynolds shear stress component: Symbols are same as Fig. 5.

profiles, Fig. 4. Furthermore, for $2.5 \leq x/h \leq 4$ without the disturbance, there is another maximum in the central side of y/b . In this downstream region, values with disturbance are larger than without it. Further downstream, values in the outer region of y/b increase little, although in the inner region they increase with the extinction of the potential core. The distribution at $x/h = 14$ is largest in the whole region of y/b , though at $x/h = 20$ they are rather smaller. The degree of these overshoots is larger without disturbance.

Figure 6 shows distributions of the rms value of the fluctuating velocity in the normal component. These distributions also increase in the downstream direction. In the region of $2 \leq x/h \leq 4$, values with disturbance are larger. Unlike u' , however, there is not another maximum value on the smaller side of y/b . Further downstream, values in the outer region of y/b increase little, although they increase in the inner region with the extinction of the potential core. In the region of $x/h > 10$, the maximum value is on the centerline. Though not shown here, the mean velocity in the normal direction, V , was anti-symmetric with respect to the centerline. This made the velocity gradient $\partial V/\partial y$ maximum on the centreline and, also, made the value of v' on the centreline maximum. The overshoot is also seen here; distribution becomes largest at $x/h = 14$ and 10 without and with the disturbance, respectively. Further downstream distributions become smaller.

Figure 7 shows distributions of Reynolds shear stress $\overline{uv'}/U_m^2$. The values increase downstream generally, and suddenly increase at $x/h = 3$ and 2 without and with disturbance, respectively. In the region of $2 \leq x/h \leq 10$, values are larger with disturbance. Near the centerline, values are approximately 0, due to the potential core. In both cases, the disturbances are almost similar in the region of $10 < x/h$. The shape there is anti-symmetric with respect to the centerline. The overshoot is also seen here; distribution becomes largest at $x/h = 14$ and 10 without and with disturbance, respectively. Further downstream distributions become smaller.

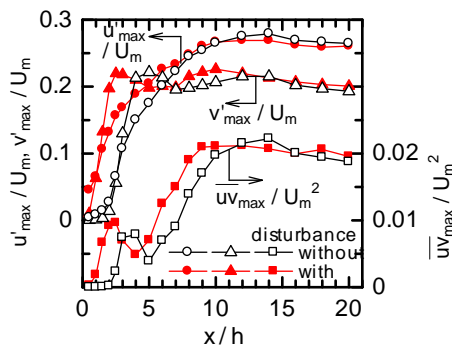


Figure 8. Downstream distribution of maximum fluctuating velocities

The above-mentioned distribution shape in the self-preservation region ($10 < x/h$) in Figs. 5-7 qualitatively accords with the results obtained in the self-preservation domain of the plane jet [4].

To show the downstream increase and overshoot of the fluctuating velocities and Reynolds shear stress clearly, the maximum values in the distribution in respective x/h are indicated in Fig. 8. The streamwise fluctuation u'_{max} increases more rapidly with disturbance in the region of $x/h \leq 2$. After the value without disturbance increased rapidly, however, the growth rate without disturbance is approximately equal to it with disturbance. This sudden increase becomes less acute at x/h is approximately 3 and 2 without and with the disturbance, respectively.

Variations in the region well away from the nozzle will be described. In the streamwise fluctuation, u'_{max} , the case without disturbance is larger in $10 < x/h$, then both become approximately equal with $x/h = 20$. In both cases, the overshoot is seen and becomes greatest in $x/h \approx 14$. In the normal fluctuation, v'_{max} , the value repeatedly decreases and increases after both disturbances reach the maximum value of about 0.22. If the distribution without disturbance is shifted upstream for $x/h \approx 2$, it almost coincides with the one with disturbance. In addition, values of both disturbances are approximately equal at $x/h = 20$. The Reynolds stress \overline{uv}_{max} decreases a little once it reaches the maximum value. In this section increase of u'_{max} becomes milder and v'_{max} becomes maximum. In other words, decrease of v component contributes to the decrease of \overline{uv}_{max} downstream. The Reynolds stress increases again, for u component keeps increasing while v component continues constant. The values that take maximum at x/h are approximately 14 and 10 without and with the disturbance, respectively. In this distribution also, if the distribution without disturbance is shifted upstream for $x/h \approx 2$, it almost coincides with the one with the disturbance.

As mentioned above, the disturbance introduced in this experiment does not affect the final values of fluctuation, although it hastens the amplification of the fluctuation.

Conclusions

Due to the disturbance introduced by the oscillating plates, just after a nozzle, periodic variation appears in the streamwise velocity whose frequency is the same as the plate oscillation frequency. The phase reverses between the neighborhood of the nozzle centerline and the neighborhood of the nozzle edge. At the normal position where the phase reverses, the power spectrum of the periodical frequency becomes smallest. The flow rate obtained by the integration over the whole section always becomes constant. At the normal position near the plate, periodic variation becomes remarkable in the normal velocity component. The phase is the same as the plate oscillation.

The maximum of the reduction rate of the exit area by the oscillation plate is only 5%, but the jet widens just after the nozzle, and the diffusion in the neighborhood of the centerline is promoted due to the increase of fluctuation.

The plate oscillation increases velocity fluctuation just after the nozzle, though the values of fluctuation become the same as without disturbance downstream. The disturbance introduced in this experiment does not affect the final values of fluctuation, although it hastens the amplification of the fluctuation. The velocity fluctuations increase downstream, then decrease a little after they reach maximum. The normal component decreases a little after having become maximum earlier than the streamwise component.

References

- [1] Browand, F. K., An Experimental Investigation of the Instability of an Incompressible, Separated Shear Layer, *J. Fluid Mech.*, **26-2**, 1966, 281-307.
- [2] Freymuth, P., On Transition in a Separated Laminar Boundary Layer, *J. Fluid Mech.*, **25-4**, 1966, 683-704.
- [3] Gaster, M., Kit, E. & Wygnanski, I., Large-Scale Structures in a Forced Turbulent Mixing Layer, *J. Fluid Mech.*, **150**, 1985, 23-39.
- [4] Heskestad, G., Hot-Wire Measurements in a Plane Turbulent Jet, *Trans. ASME, J. Appl. Mech.*, **32-4**, 1965, 721-734.
- [5] Hsiao, F.-B. & Huang, J.-M., Near-Field Flow Structures and Sideband Instabilities of an Initially Laminar Plane Jet, *Expts. Fluids.*, **9-1~2**, 1990, 2-12.
- [6] Huang, L.-S. & Ho, C.-M., Small-scale transition in a Plane Mixing Layer, *J. Fluid Mech.*, **210**, 1990, 475-500.
- [7] Husain, H.S. & Hussain, F., Experiments on Subharmonic Resonance in a Shear Layer, *J. Fluid Mech.*, **304**, 1995, 343-372.
- [8] Michalke, A., Vortex Formation in a Free Boundary Layer According to Stability Theory, *J. Fluid Mech.*, **22-2**, 1965, 371-383.
- [9] Michalke, A., On Spatially Growing Disturbances in an Inviscid Shear Layer, *J. Fluid Mech.*, **23-3**, 1965, 521-544.
- [10] Miksad, R.W., Experiments on the Nonlinear Stages of Free-Shear-Layer Transition, *J. Fluid Mech.*, **56-4**, 1972, 695-719.
- [11] Sato, H., Further Investigation on the Transition of Two-Dimensional Separated Layer at Subsonic Speeds, *J. Phys. Soc. Jpn.*, **14-12**, 1959, 1797-1810.
- [12] Sato, H., The Stability and Transition of a Two-Dimensional Jet, *J. Fluid Mech.*, **7**, 1960, 53-80.